C. R. Mecanique 342 (2014) 478–484

Contents lists available at ScienceDirect

Comptes Rendus Mecanique

www.sciencedirect.com

Development of secondary flows in viscoelastic curved ducts and the influence of outlet region

Développement de l'écoulement secondaire dans les conduites courbées et influence de la région de sortie pour un fluide viscoélastique

Gilmar Mompean [a,*], Tibisay Coromoto Zambrano [b], Zaynab Salloum [c]

[a] *Laboratoire de mécanique de Lille, UMR CNRS 8107, Polytech-Lille, Cité scientifique, 59665 Villeneuve-d'Ascq cedex, France*
[b] *Université centrale du Venezuela, Cité universitaire, 1053 Caracas, Venezuela*
[c] *Université libanaise, Laboratoire des mathématiques–EDST, Hadath, Lebanon*

ARTICLE INFO

Article history:
Received 31 March 2014
Accepted 29 April 2014
Available online 2 July 2014

Keywords:
Dean vortex
Deborah number
Viscoelastic flow simulation
Curved duct

Mots-clés :
Vortex de Dean
Nombre de Deborah
Simulation de fluide viscoélastique
Conduite courbée

ABSTRACT

This paper presents numerical simulations of Newtonian and viscoelastic flows through a 180° curved duct of square cross section with a long straight outlet region. A particular attention is paid to the development of the flow in the output rectangular region after the curved part. The viscoelastic fluid is modeled using the constitutive equation proposed by Phan–Thien–Tanner (PTT). The numerical results, obtained with a finite-volume method, are shown for three different Dean numbers (125, 137, 150) and for three Deborah numbers (0.1, 0.2, 0.3). The necessary outlet length to impose boundary conditions is presented and discussed for these cases. Streamlines and vortex formation are shown to illustrate and analyze the evolution of the secondary flow in this region.

RÉSUMÉ

Ce travail présente des résultats numériques concernant l'étude des fluides newtoniens et viscoélastiques passant par une conduite courbée à 180°, de section carrée, avec une longue zone droite de sortie. Une attention particulière est portée à l'analyse de l'écoulement dans la région rectangulaire de sortie après la partie incurvée. Le fluide viscoélastique est modélisé à l'aide de l'équation constitutive proposée par Phan–Thien–Tanner (PTT). Les résultats numériques, obtenus avec la méthode des volumes finis, sont présentés pour trois nombres de Dean (125, 137, 150) et pour trois nombres de Deborah (0, 1, 0, 2, 0, 3). La longueur du domaine de calcul nécessaire pour bien imposer les conditions aux limites de sortie est présentée et discutée. Les lignes de courant montrant la formation de l'écoulement secondaire sont montrées pour illustrer le comportement de l'écoulement dans cette région.

* Corresponding author.
E-mail addresses: gilmar.mompean@polytech-lille.fr (G. Mompean), tc.zambrano@ed.univ-lille1.fr (T.C. Zambrano), salloum@ul.edu.lb (Z. Salloum).

http://dx.doi.org/10.1016/j.crme.2014.04.003
1631-0721/

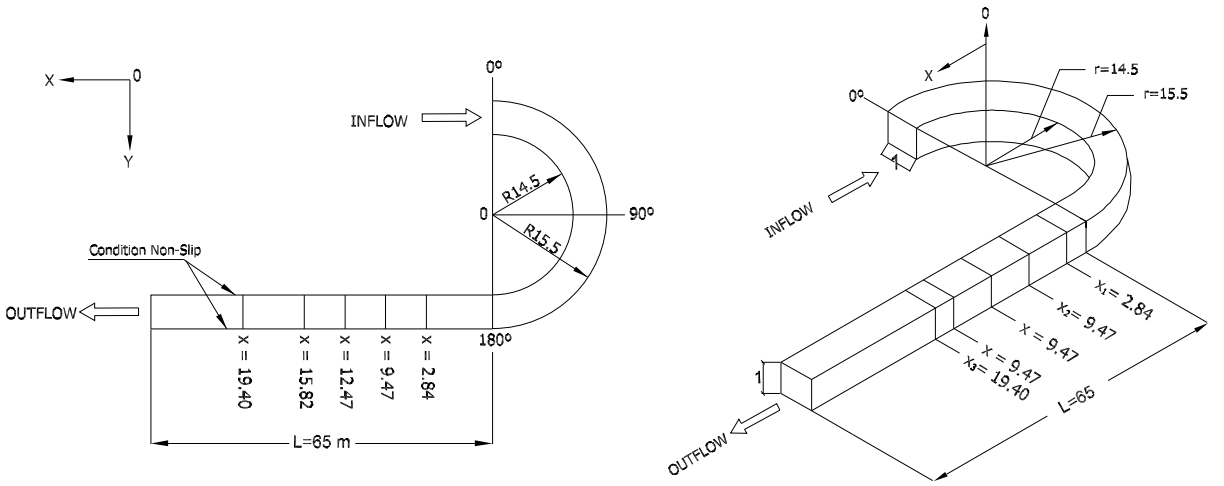

Fig. 1. Geometry.

1. Introduction

The study of Newtonian and viscoelastic flows through complex geometries is an important topic of research and has several practical applications. In this work, we consider a curved channel of 180°, which is widely applied in several domains of engineering and presents a scientific interest for the understanding of the presence and development of secondary flows in curved ducts. This kind of geometry can be found in different industrial applications, to cite a few: petroleum or petrochemical industry, injection of polymeric materials, heat exchangers, biomedical systems, etc.

The work of Dean [1] is the basis of several researches on the behavior of Newtonian flows through curved channels with square cross section. He analyzed the formation of vortex in a curved channel with the perturbation method for a Newtonian fluid. He was the first to demonstrate the appearance of twin counterrotating vortices in the curved part of a channel, which are the result of the interaction between inertia, viscous and centrifugal forces. Dean introduced a dimensionless number, which represents the ratio between the centrifugal forces and the viscous forces, and is related to the intensity of secondary flows. This number has been called Dean number, Dn, and is defined as

$$Dn = Re\sqrt{\frac{a}{R_2}} \tag{1}$$

where a the characteristic length associated with the cross section of the channel, R_2 is the radius of the external curvature of the channel, and Re is the Reynolds number based on the bulk velocity and on the length a.

Berger et al. [2] performed an extensive review of the topic for Newtonian fluids. Bara et al. [3] performed an experimental study for incompressible Newtonian flows through a curved duct with square cross section, and demonstrated the appearance of more than one pair of vortices as secondary flow. Bhunia and Cheng [4] studied the behavior of an air flow through a curved rectangular channel with a variable cross section. They showed that a secondary motion sets in radial direction of the curved section, which in combination with the axial flow leads to the formation of a base vortex. There are only few works in this field considering the secondary flows in curved ducts for viscoelastic fluids (Helin et al. [5] and Boutabaa et al. [6]).

The originality of this work is to use a large extension of the straight output zone (after the curved part, as shown in Fig. 1) considering different Dean and Deborah numbers. The Phan–Thien–Tanner (PTT) constitutive equation is used to model the viscoelastic fluid. Preliminary results were presented in a conference (see [7]), and in the present paper our aim is to study in details the persistence of the secondary flow in this straight part of the outlet region. The numerical simulations are done for a three-dimensional computational domain, considering Newtonian and viscoelastic fluids. The secondary flow is observed in the normal direction (perpendicular to the streamwise direction) of the main flow through a U-curved channel of 180° of square cross section, for three Dean numbers $Dn = 125$, 137, and 150, and three Deborah numbers $De = 0.1$, 0.2 and 0.3. The Deborah number is defined as $De = \lambda U/a$, where λ is the relaxation time of the viscoelastic fluid, U the bulk velocity and a the height of the channel. The length of the outlet region of the channel was extended up to $65a$. Fig. 1 shows the geometrical configuration. The results are obtained using a finite-volume numerical method written in general orthogonal coordinates with a staggered grid [8]. The analysis was performed using the velocity field and streamlines.

The paper is organized as follows. Section 2 presents the governing equations; the numerical method and the geometry description are briefly described in Section 3, and the results and the conclusions are presented and analyzed respectively in Sections 4 and 5.

2. Governing equations

The governing equations are written for mass and momentum conservation considering the fluid as incompressible and non-Newtonian.

- i) Mass conservation:

$$\nabla \cdot \mathbf{v} = 0 \tag{2}$$

where $\mathbf{v}$ is the velocity vector and ∇ the nabla operator.

- ii) Momentum conservation:

$$\rho(\mathrm{D}\mathbf{v}/\mathrm{D}t) = \nabla \cdot (-p\mathbf{I} + 2\eta_s\mathbf{D} + \boldsymbol{\tau}) \tag{3}$$

where $\mathrm{D}/\mathrm{D}t$ is the material derivative, ρ the fluid density, p the pressure, $\mathbf{I}$ the identity matrix, η_s the solvent viscosity, $\boldsymbol{\tau}$ the polymeric contribution to the extra-stress tensor and $\mathbf{D} = 1/2(\nabla\mathbf{v} + \nabla\mathbf{v}^{\mathbf{T}})$ the rate-of-deformation tensor. The constitutive equation of Phan–Thien–Tanner (PTT) is used to model the extra-stress polymeric components $\boldsymbol{\tau}$.

- iii) Constitutive equation of PTT model:

$$f\big(\{\boldsymbol{\tau}\}\big)\boldsymbol{\tau} + \lambda\big[\big(\mathrm{D}\boldsymbol{\tau}/\mathrm{D}t - \boldsymbol{\tau}\nabla\mathbf{v} - \nabla\mathbf{v}^{\mathbf{T}}\boldsymbol{\tau}\big)\big] = 2\eta_p\mathbf{D} \tag{4}$$

where the function $f(\{\boldsymbol{\tau}\})$ is defined as

$$f\big(\{\boldsymbol{\tau}\}\big) = \exp(\varepsilon\lambda/\eta_p)\{\boldsymbol{\tau}\} \tag{5}$$

η_p represents the polymeric viscosity, $\{\boldsymbol{\tau}\}$ the trace tensor $\boldsymbol{\tau}$, λ the relaxation time and ε a parameter characterizing the elongational behavior of the model. It is noted that when $f(\{\boldsymbol{\tau}\})$ is equal to 1, the PTT model reduces to the Oldroyd-B model.

2.1. Governing equations in general orthogonal coordinates

The behavior of the fluid flow is described by the mass conservation equation (Eq. (2)) and by the momentum conservation equation (Eq. (3)) and, for the case of viscoelastic fluids, the constitutive equation of Phan–Thien–Tanner is also included in the governing equations. In order to model the curved part of the duct, the procedure proposed by Pope [9] to transform the transport equations from the Cartesian form into the generalized orthogonal coordinates through geometric transformations is used. In this work, the conservation and constitutive equations are expressed in terms of general orthogonal coordinates. Let us consider the orthogonal coordinate transformation from Cartesian coordinates using the initial notation, x_i, to curvilinear coordinates ψ_i, where $i = 1, 2, 3$. The spatial derivatives will be expressed in terms of the physical infinitesimal variations of length, $\mathrm{d}\xi_i = h_i\mathrm{d}\psi_i$, where $h_i = \sqrt{g_{ii}}$ denotes the scale factors written in terms of the ith component of the diagonal metric tensor. The physical curvilinear velocity field is defined by $V_i = h_i v^i$, such that $v^i = \mathrm{d}\psi_i/\mathrm{d}t$. Below is presented a brief description of the procedure, for details see also [8]. The mass conservation equation for an incompressible flow can be written as:

$$\sum_i \nabla_{\cdot(i)}\,(V_i) = \sum \frac{\partial V_i}{\partial \xi_i} + \sum_{j\neq i} H_i^j V_i = 0 \tag{6}$$

where $H_i^j = \frac{1}{h_i}\frac{\partial h_i}{\partial \xi_j}$ are the Christoffel symbols.

In particular, we can also define the components L_{ij} of the generalized velocity gradient $\mathbf{L}$, by $L_{ij} = \frac{\partial V_j}{\partial \xi_i} - H_i^j V_i + \sum_k H_j^k V_k \delta_{ij}$, with δ_{ij} Kronecker's delta. The momentum conservation equation is given by:

$$\frac{\partial(\rho V_j)}{\partial t} + \sum_i \nabla_{\cdot(i)}(\rho V_i V_j - \mathcal{T}_{ij}) = -\frac{\partial p}{\partial \xi_j} - \sum_i H_j^i(\rho V_i V_j - \mathcal{T}_{ij}) + \sum_i H_i^j(\rho V_i V_i - \mathcal{T}_{ii}) \tag{7}$$

with $\mathcal{T}_{ij} = \tau_{ij} + 2\eta_s D_{ij}$, where τ_{ij} represent the physical components of the extra-stress tensor $\mathbf{T}$, η_s the solvent Newtonian viscosity and D_{ij} the components of the rate-of-deformation tensor $\mathbf{D} = \frac{1}{2}(\mathbf{L} + \mathbf{L}^{\mathrm{T}})$.

The constitutive equation of the PTT model in general orthogonal coordinates results from the transformation of the second-order tensor arising from advection of the extra-stress tensor:

$$\begin{aligned} f\big(\{\mathbf{T}\}\big)\tau_{ij} + \lambda\Bigg\{ &\frac{\partial \tau_{ij}}{\partial t} + \sum_k \nabla_{\cdot(k)}\,(V_k\tau_{ij}) - \sum_k H_k^i V_k \tau_{kj} + \sum_k H_i^k V_i \tau_{kj} - \sum_k H_k^j V_k \tau_{ik} \\ &+ \sum_k H_j^k V_j \tau_{ik} - \sum_k L_{ik}\tau_{kj} - \sum_k L_{jk}\tau_{ki}\Bigg\} = 2\eta_p D_{ij} \end{aligned} \tag{8}$$

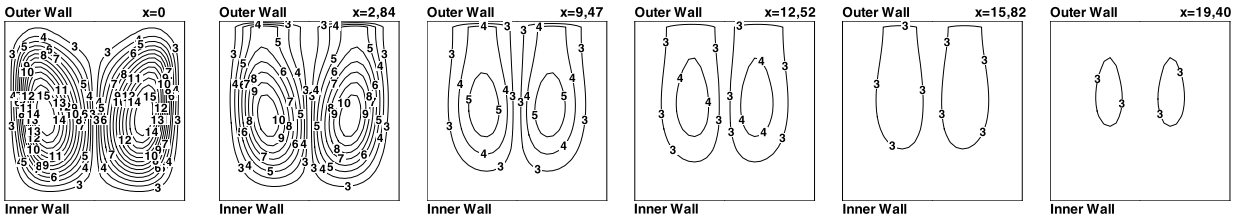

Fig. 2. Streamlines of the Newtonian flow in cross section at positions $x = 0$, $x = 2.84$, $x = 9.47$, $x = 12.52$, $x = 15.82$, and $x = 19.40$ for $Dn = 125$. (Scale: max = 1.3E–02; min = −1.10E–03; $\Delta = 0.001$.)

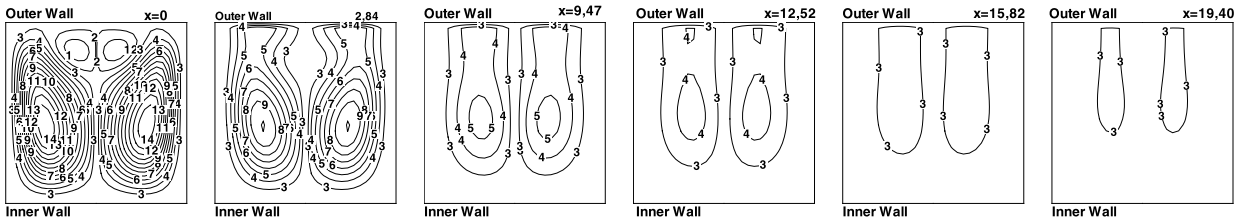

Fig. 3. Streamlines of the Newtonian flow in cross section at positions $x = 0$, $x = 2.84$, $x = 9.47$, $x = 12.52$, $x = 15.82$, and $x = 19.40$ for $Dn = 137$. (Scale: max = 1.3E–02; min = −1.10E–03; $\Delta = 0.001$.)

where η_p is the polymeric viscosity and $f(\{\mathbf{T}\})$ is function of the trace $\{\mathbf{T}\}$ of the extra-stress tensor $\mathbf{T}$, depending on the dimensionless material parameter characterizing the elongational behavior of model and the zero-shear rate polymeric viscosity.

3. Numerical method and geometry description

The method used to solve the system of equations in general orthogonal coordinates is the finite-volume method. The equations are integrated in a control volume, and then the Gauss theorem is used to transform the volume integrals into surface integrals. The staggered-grid approach is used to define the locations of the primitive variables (velocity, pressure, and extra-stresses). The numerical algorithm used is based on Marker and Cell approach proposed by Harlow and Welch [11]. The velocity field is solved explicitly with an implicit Poisson solver for pressure. The Poisson equation is then solved using a Cholesky direct method or a preconditioned conjugate gradient method. The advection terms are discretized using a second-order scheme (QUICK, from Leonard [10]). The advance in time is obtained by a first-order Euler scheme. A three-dimensional flow of Newtonian and viscoelastic fluids through a curved channel with a square cross-section is considered. The classical boundary conditions are employed for this geometry: no-slip at the walls, developed velocity profile in the inlet and uniform pressure at the outlet section.

4. Results

The results presented in this work are obtained for Newtonian and viscoelastic flows for three Dean numbers $Dn = 125$, 137, and 150, and for three Deborah numbers ($De = 0.1$, 0.2 and 0.3) when the viscoelastic fluid is considered. Results are presented for the developing region after the curved part, where the coordinate $x = 0$ corresponds to the origin of the straight part of the outlet duct. Fig. 1 illustrates the geometrical configuration and the sections used to analyze the flow. The following positions of the cross sections were selected to follow the development of the secondary flow: $x = 0$, $x = 2.84$, $x = 9.47$, $x = 12.52$, $x = 15.82$, and $x = 19.40$. The evolution of the secondary flow is presented using the streamline functions. The results are presented and analyzed in the straight part, just after the curved part, showing the development of the counterrotating vortices along these cross sections.

4.1. Newtonian flow

The first case considered in this work is the Newtonian flow at $Dn = 125$. For this Dean number, we observe the presence of two counterrotating vortices, as shown in Fig. 2. Their size and intensity decrease as the flow is developing from $x = 0$ up to $x = 19.40$. As will be shown, at this Dean number the centrifugal forces are not large enough to create additional vortices.

When $Dn = 137$, the centrifugal force is greater than the case when $Dn = 125$, and an additional pair of vortices is clearly seen (see Fig. 3, when $x = 0$). This pair of vortices is only observed at the beginning of the straight part of the channel. In the next cross section ($x = 2.84$) the influence of this new pair of vortices is modifying the streamlines of the main pair. After this section, the two standard counterrotating vortices become weaker, dissipating their energy (as in the previous Dn number case).

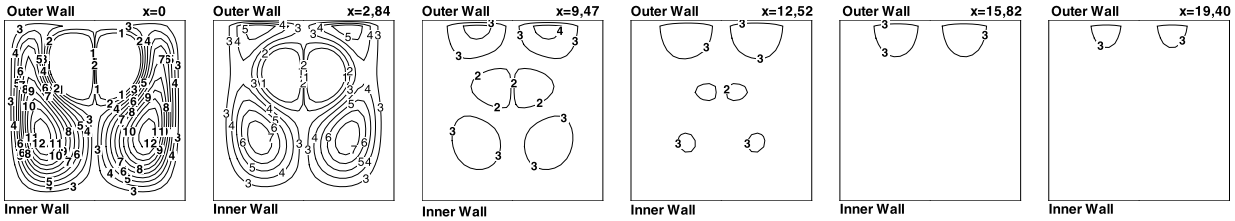

Fig. 4. Streamlines of the Newtonian flow in cross section at positions $x = 0$, $x = 2.84$, $x = 9.47$, $x = 12.52$, $x = 15.82$, and $x = 19.40$ for $Dn = 150$. (Scale: max = 1.3E–02; min = −1.10E–03; $\Delta = 0.001$.)

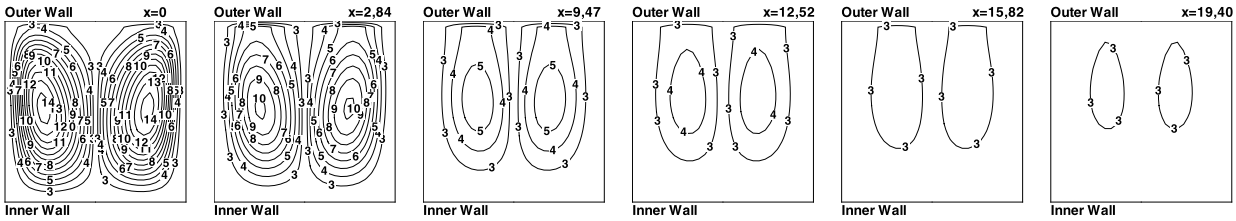

Fig. 5. Streamlines of the non-Newtonian flow in cross section at positions $x = 0$, $x = 2.84$, $x = 9.47$, $x = 12.52$, $x = 15.82$, and $x = 19.40$ for $Dn = 125$ and $De = 0.1$. (Scale: max = 1.3E–02; min = −1.10E–03; $\Delta = 0.001$.)

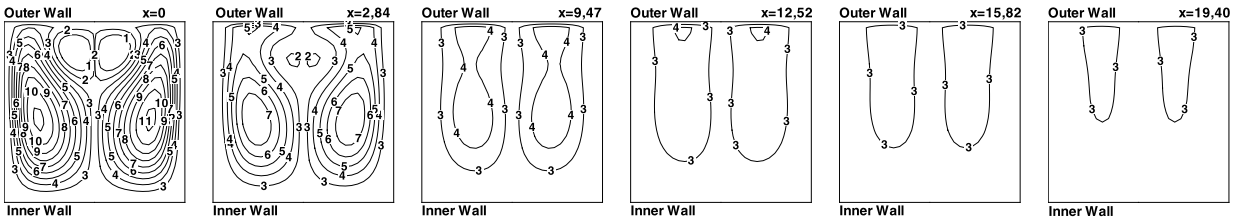

Fig. 6. Streamlines of the non-Newtonian flow in cross section at positions $x = 0$, $x = 2.84$, $x = 9.47$, $x = 12.52$, $x = 15.82$, and $x = 19.40$ for $Dn = 125$ and $De = 0.2$. (Scale: max = 1.3E–02; min = −1.10E–03; $\Delta = 0.001$.)

For the case at $Dn = 150$, shown in Fig. 4, centrifugal forces are stronger, so the transition of two counterrotating vortices to four counterrotating vortices is clearly seen. In addition, we observe the presence of two new counterrotating vortices, which modify the pattern of four cells to six cells (from section $x = 2.84$ up to $x = 12.52$). Then, after this section ($x = 12.52$) this pattern is dissipated as the flow develops.

For all cases, the total length of the outlet region (straight part) used for the numerical simulations was $L = 65$ (65 times the height of the square duct). The results show that after $x = 19.40$, the flow is completely developed. After this cross section, the secondary flow is no more influenced by the curved part of the channel.

4.2. Viscoelastic flow

For the analysis of the viscoelastic flow, the constitutive equation of Phan–Thien–Tanner (PTT model) is used to model the fluid, and the Deborah numbers chosen are $De = 0.1$, 0.2, and 0.3. This allows us to study the influence of the fluid's elasticity in the evolution of the secondary flow. In order to keep the same level of inertia and curvature in the comparison between the Newtonian and the viscoelastic cases, the same three Dean numbers ($Dn = 125$, 137 and 150) are employed here for the viscoelastic flow.

Fig. 5 shows the streamlines for the case when $Dn = 125$ and $De = 0.1$. A similar vortex structure is observed as for the Newtonian case, showing that for this De number the elasticity has little influence in the development of the secondary vortices. In fact, a twin counterrotating vortex is maintained along the straight outlet region of the channel.

Keeping the same Dean number ($Dn = 125$), and increasing the Deborah number ($De = 0.2$), we noted that at the exit of the curved zone appears a new pair of counterrotating vortices as illustrated in Fig. 6 ($x = 0$). This new pair of counterrotating vortices dissipates along the straight outlet channel, and disappears completely at section $x = 12.52$. Increasing now the Deborah number ($De = 0.3$) and keeping the same Dean number ($Dn = 125$), the size and the intensity of the four counterrotating vortices become more important, and this vortex pattern is observed up to the section $x = 15.82$, as shown in Fig. 7. After this section we observed the presence of only two weak vortices.

Increasing the Dean number to $Dn = 137$, we clearly see four vortices at the beginning of the straight duct part for all the cases (three Deborah numbers $De = 0.1$, 0.2 and 0.3), as shown respectively in Figs. 8, 9 and 10. For these cases, there is a remarkable difference when the Deborah number increases from 0.1 to 0.2. The four-vortex pattern is presented up to

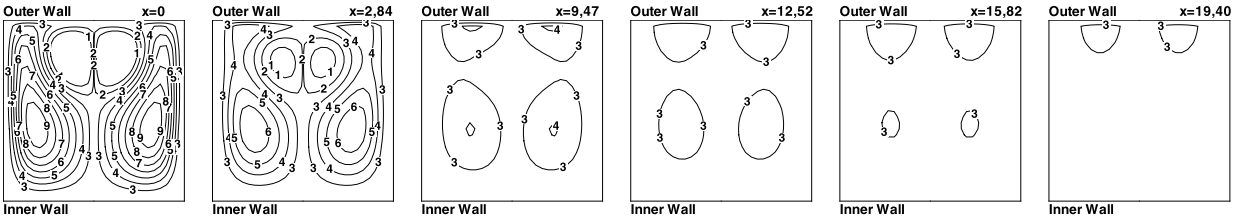

Fig. 7. Streamlines of the non-Newtonian flow in cross section at positions $x = 0$, $x = 2.84$, $x = 9.47$, $x = 12.52$, $x = 15.82$, and $x = 19.40$ for $Dn = 125$ and $De = 0.3$. (Scale: max = 1.3E–02; min = −1.10E–03; $\Delta = 0.001$.)

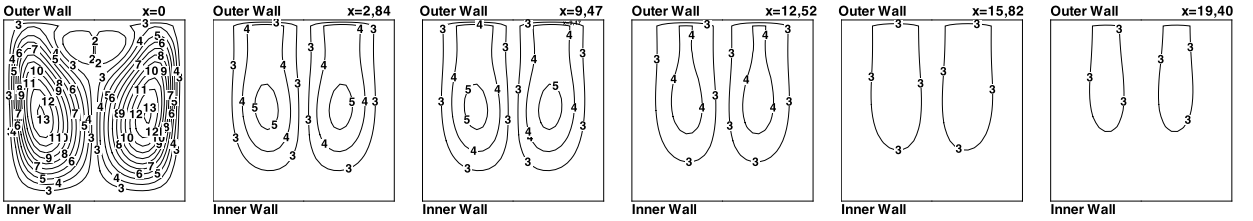

Fig. 8. Streamlines of the non-Newtonian flow in cross section at positions $x = 0$, $x = 2.84$, $x = 9.47$, $x = 12.52$, $x = 15.82$, and $x = 19.40$ for $Dn = 137$ and $De = 0.1$. (Scale: max = 1.3E–02; min = −1.10E–03; $\Delta = 0.001$.)

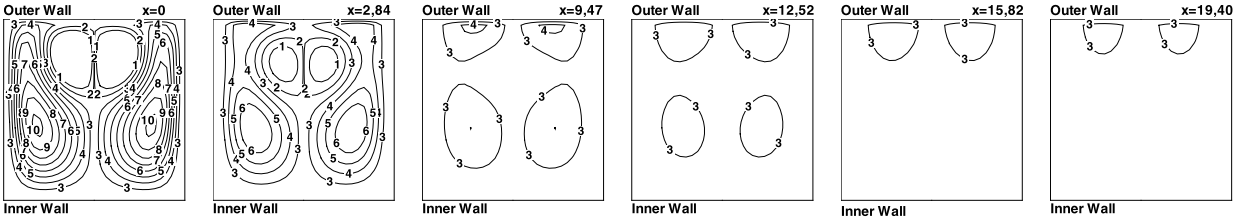

Fig. 9. Streamlines of the non-Newtonian flow in cross section at positions $x = 0$, $x = 2.84$, $x = 9.47$, $x = 12.52$, $x = 15.82$, and $x = 19.40$ for $Dn = 137$ and $De = 0.2$. (Scale: max = 1.3E–02; min = −1.10E–03; $\Delta = 0.001$.)

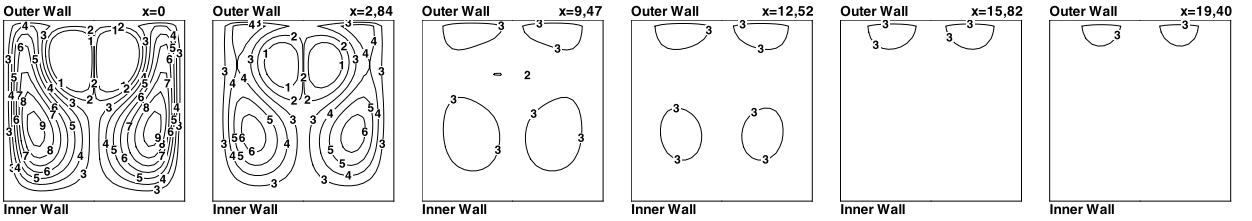

Fig. 10. Streamlines of the non-Newtonian flow in cross section at positions $x = 0$, $x = 2.84$, $x = 9.47$, $x = 12.52$, $x = 15.82$, and $x = 19.40$ for $Dn = 137$ and $De = 0.3$. (Scale: max = 1.3E–02; min = −1.10E–03; $\Delta = 0.001$.)

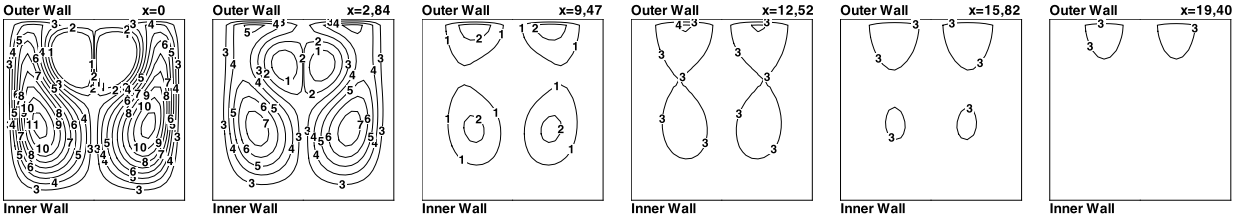

Fig. 11. Streamlines of the non-Newtonian flow in cross section at positions $x = 0$, $x = 2.84$, $x = 9.47$, $x = 12.52$, $x = 15.82$, and $x = 19.40$ for $Dn = 150$ and $De = 0.1$. (Scale: max = 1.3E–02; min = −1.10E–03; $\Delta = 0.001$.)

the section $x = 12.52$. The same qualitative behavior is observed when $De = 0.3$ (see Figs. 9 and 10). However, for $De = 0.1$ (Fig. 8), the four-vortex pattern was observed only at the exit of the curved zone.

Finally, in Figs. 11, 12, and 13 is shown the behavior of the secondary flow for $Dn = 150$ at $De = 0.1$, 0.2 and 0.3, respectively. For this Dean number, in the section $x = 0$, at the beginning of the straight part, the four-vortex pattern is presented for all Deborah numbers up to section $x = 2.84$. We observe an interesting behavior for this Dean number when

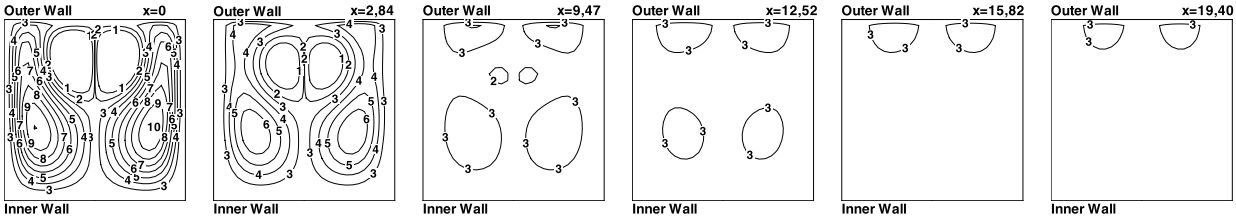

Fig. 12. Streamlines of the non-Newtonian flow in cross section at positions $x = 0$, $x = 2.84$, $x = 9.47$, $x = 12.52$, $x = 15.82$, and $x = 19.40$ for $Dn = 150$ and $De = 0.1$. (Scale: max = 1.3E–02; min = −1.10E–03; $\Delta = 0.001$.)

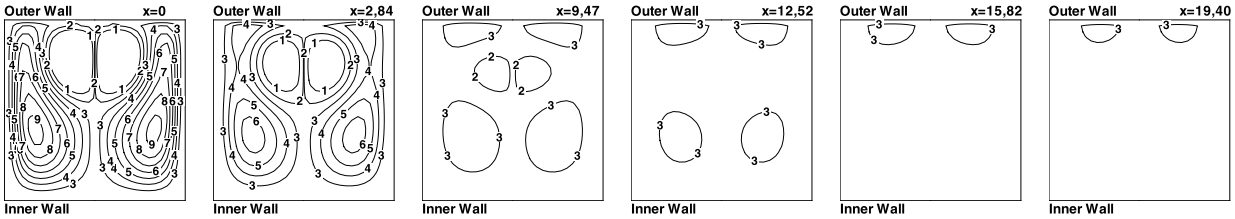

Fig. 13. Streamlines of the non-Newtonian flow in cross section at positions $x = 0$, $x = 2.84$, $x = 9.47$, $x = 12.52$, $x = 15.82$, and $x = 19.40$ for $Dn = 150$ and $De = 0.3$. (Scale: max = 1.3E–02; min = −1.10E–03; $\Delta = 0.001$.)

the Deborah number increases, with the appearance of six vortices, as shown in Figs. 12 and 13 at the section $x = 9.47$. For all studied viscoelastic cases presented in this work, the length corresponding to $x = 19.40$ was enough to dissipate the secondary flows.

5. Conclusions

This study was performed to analyze the different behaviors of Newtonian and viscoelastic fluids when flowing throughout a 180° curved duct of square cross section. The viscoelastic fluid was modeled using the Phan–Thien–Tanner (PTT) constitutive equation. The conservation (mass and momentum) and the constitutive equations were solved using a second-order finite-volume method. In order to verify the behavior of the vortex evolution after the curved part, a long straight outlet part of the duct was employed to allow the complete development of the flow is this part.

For the study of the viscoelastic flow, three Dean numbers ($Dn = 125$, 137 and 150) and also three Deborah numbers ($De = 0.1$, 0.2 and 0.3) were considered. The Newtonian flows for the same Dean numbers were also presented in order to compare and verify the influence of the elasticity of the viscoelastic fluid in the pattern of the secondary flow. The study shows that the number of vortices that appears as secondary flows in the straight part of the curved channel depends also on Dean and Deborah numbers.

For the Newtonian fluid, it is shown that the number of vortices is related with the Dean number. For Dean numbers $Dn = 125$, 137 and 150, one observes the apparition of two, four, and six vortices, respectively. For the viscoelastic flows, the increase of the elasticity of the fluid (represented by the Deborah number) is an important parameter for the transition and the increase of secondary flow characteristics. For the studied cases, the results also show that after around 20 channel height ($x = 19.40$), the flow can be considered completely developed. Further studies are needed to verify the influence of the length of the straight channel output for higher Dean and Deborah numbers, and check how the first normal stress difference can be related with the evolution of secondary flows.

References

[1] W.R. Dean, Fluid motion in a curved channel, Proc. R. Soc. Lond. Ser. A 121 (1928) 402–420.
[2] S.A. Berger, L. Talbot, L.-S. Yao, Flow in curved pipes, Annu. Rev. Fluid Mech. 15 (1983) 461–512.
[3] B. Bara, K. Nandakumar, J.H. Masliyah, An experimental and numerical study of the Dean problem: flow development towards two-dimensional multiple solutions, J. Fluid Mech. 244 (1992) 339–376.
[4] A. Bhunia, C.L. Chen, Flow characteristics in a curved rectangular channel with variable cross-sectional area, J. Fluids Eng. 131 (2009) 1–17.
[5] L. Helin, L. Thais, G. Mompean, Numerical simulation of viscoelastic Dean vortices in a curve duct, J. Non-Newton. Fluid Mech. 156 (2009) 84–94.
[6] M. Boutabaa, L. Helin, G. Mompean, L. Thais, Numerical study of Dean vortices in developing Newtonian and viscoelastic flows through a curved duct of square cross-section, C. R. Mecanique 337 (2009) 40–47.
[7] T. Zambrano, G. Mompean, Z. Salloum, Numerical study of a viscoelastic fluid in the output region of curved duct using a finite volume method, in: 11th International Conference of Numerical Analysis and Applied Mathematics, ICNAAM 2013, Rhodes, Greece, 21–27 September 2013, in: AIP Conf. Proc., vol. 1558, 2013, p. 1414.
[8] G. Mompean, L. Thais, Finite volume simulation of viscoelastic flows in general orthogonal coordinates, Math. Comput. Simul. 80 (2010) 2185–2199.
[9] S.B. Pope, The calculation of turbulent recirculating flows in general orthogonal coordinates, J. Comput. Phys. 26 (1978) 197–217.
[10] B. Leonard, A stable accurate convective modeling procedure based on quadratic upstream interpolation, Comput. Methods Appl. Mech. Eng. 19 (1979) 59–98.
[11] F.H. Harlow, J.E. Welch, Numerical calculation of time-dependent viscous incompressible flow of fluid with free surface, Phys. Fluids 8 (1965) 2182–2189.